Supplemental Materials

Title: Radiation-induced phosphorylation of a prion-like domain regulates transformation by FUS-CHOP

Authors: Mark Chen[1,2], Joseph P. Foster II[3], Ian C. Lock[1], Nathan H. Leisenring[1], Andrea R. Daniel[4], Warren Floyd[1,2], Eric S. Xu[4], Ian J. Davis[5,6], and David G. Kirsch[1,4,*]

Affiliations:

[1]Department of Pharmacology and Cancer Biology, Duke University Medical Center, Durham, North Carolina, 27708

[2]Medical Scientist Training Program, Duke University Medical Center, Durham, North Carolina, 27708

[3]Curriculum in Bioinformatics and Computational Biology, University of North Carolina at Chapel Hill, Chapel Hill, North Carolina, 27599

[4]Department of Radiation Oncology, Duke University Medical Center, Durham, North Carolina, 27708

[5]Lineberger Comprehensive Cancer Center, University of North Carolina at Chapel Hill, Chapel Hill, North Carolina, 27599

[6]Departments of Pediatrics and Genetics, University of North Carolina at Chapel Hill, Chapel Hill, North Carolina, 27599

*Correspondence to: David G. Kirsch, E-mail: david.kirsch@duke.edu, Tel: 919-681-8605

Duke University Medical Center, DUMC Box 91006, Durham, North Carolina 27708

Methods

RESOURCE AVAILABILITY

Lead Contact: Further information and requests for resources and reagents should be directed to and will be fulfilled by the Lead Contact, David Kirsch (david.kirsch@duke.edu).

Materials Availability: Plasmids generated in this study are available upon request.

Data and Code Availability: All genomic data underlying the study are available/will be deposited at https://www.ncbi.nlm.nih.gov/geo/query/acc.cgi?acc=GSE145678 Access will be made public after publication. For private access to these data by reviewers, please use this token: ovyxuiyebjepvaz

EXPERIMENTAL MODEL DETAILS

Plasmids and Vectors

FUS-CHOP WT, FUS-CHOP 12A, and FUS-CHOP 12E constructs were designed in Snapgene and synthesized by Genscript. The cDNA fragments were then subcloned into N174-MCS (Puro) vector backbone, which was a gift from Adam Karpf (Addgene plasmid # 81068 ; http://n2t.net/addgene:81068 ; RRID:Addgene_81068). shRNA sequences from the RNAi consortium were obtained from the Sigma-Aldrich shRNA database and shRNA oligos were ordered from Integrated DNA Technologies (IDT). shRNAs were subcloned into Tet-pLKO-puro, which was a gift from Dmitri Wiederschain (Addgene plasmid # 21915 ; http://n2t.net/addgene:21915 ; RRID:Addgene_21915) (Wiederschain et al., 2009).

Tissue culture and cell line generation

NIH-3T3 cell lines were purchased from ATCC (CRL-1658) and cultured in DMEM media (ThermoFisher Scientific, 11965092) supplemented with 10% fetal bovine serum (ThermoFisher Scientific, 16000044) and 1% antibiotic–antimycotic (ThermoFisher Scientific, 10091148), and incubated at 37°C with 5% CO2 in a humidified cell-culture incubator. Tumor cells were isolated from primary mouse sarcomas as previously described(Chen et al., 2019). Briefly, tumor tissue was minced in the cell-culture hood and digested by dissociation buffer in PBS (ThermoFisher Scientific, 14040133) containing collagenase type IV (5 mg/ml, ThermoFisher Scientific, 17104-019), dispase (1.3 mg/ml, ThermoFisher Scientific, 17105-041) as well as trypsin (0.05%, ThermoFisher Scientific, 25200056) for about 1 h at 37°C. Cells were washed with PBS (ThermoFisher Scientific, 10010023) and filtered using a 40 mm sieve (Corning, 431750), and cultured for at least four passages to deplete stroma before being used for experiments. The SW872 cell line was purchased from ATCC. MLPS cell lines MLS402 and MLS1765 were gifts from Pierre Åman (University of Gothenburg, Sweden), and the DL-221 cell line was a gift from Keila Torres and Alexander Lazar (University of Texas MD Anderson Cancer Center, Houston , Texas). SW872, MLS402 and MLS1765 were cultured in RPMI with 10% FBS and 1% antibiotic-antimycotic. Inducible shRNA cell lines were cultured in DMEM with 10% Tet-free FBS (Takara) and 1% antibiotic-antimycotic, or RPMI with 10% Tet-free FBS (Takara) and 1% antibiotic-antimycotic. DL-221 and all other cell lines were cultured in DMEM with 10% FBS and 1% antibiotic-antimycotic.

BIOINFORMATICS METHODS

ChIP-seq Analysis

Adaptor sequences were removed from reads with cutadapt (v.1.12). FASTX-Toolkit (v0.0.12) with options -Q 33, -p 90, and q 20 was used to filter reads. Reads were aligned to the hg19 genome using STAR (v2.5.2b) with the following options: --outFilterMismatchNmax 2, --chimSegmentMin 15, --chimJunctionOverhangMin 15, --outSAMtype BAM Unsorted, --outFilterType BySJout, --outFilterScoreMin 1, --outFilterMultimapNmax 1. Tracks of FUS-CHOP were created by visualizing RPM normalized bigWigs on UCSC genome browser. FUS-CHOP regions of enrichment (ROE) were identified using MACS2 (v2.1.2) using default parameters and cell line matched input samples as controls. For each ROE identified by MACS2 a score per million (SPM) was calculated, and low confidence peaks (bottom 5% of SPM scores) were removed for downstream analysis(16). FUS-CHOP ROE was defined as +/- 90 bp MACS2 identified summit. The +/- 90 bp window size was determined empirically by calculating the ratio of the number of overlapping FUS-CHOP ROE summits found in the MLS402 and DL221 cell line over the total number of MLS402 ROE as a variable window was added to ROE summits found in the MLS402 cell line. A 180 bp window was selected for downstream analysis as an increase in the window size did not increase the overlapping number of ROE. Annotating FUS-CHOP ROE with genomic features was done using the HOMER annotatePeaks.pl with the options hg19 (v4.10.3). FUS-CHOP ROE-enhancer set was defined by excluding any FUS-CHOP ROE that fell with a gene promoter region (+300:Ref-seqTSS:-500 bp – longest transcript). Average line plot signal for FUS-CHOP and H3K27ac in MLS402, DL221, and SW872 cells was isolated using deepTools (v3.2.0). Signal shown in heatmaps was log2 transformed, and the max signal was set at the 99th percentile across MLS402, DL221, and

SW872 cell lines. Motifs found at FUS-CHOP ROE were identified using HOMER (v4.10.3) using HOMER defined random background regions. GREAT (17) was used to annotate ChIP-seq ROE with associated genes. All visualizations were created using Python. Any ChIP-seq intersection set was identified using bedtools (v2.28.0).

CUT&RUN Analysis

Adaptor sequences were removed using (cutadapt v1.12), and reads were then quality filtered using fastq quality filter in FASTX-Toolkit (v0.0.12) with options -Q 33, -p 90, and q 20. Reads were aligned to a custom hg19-eColi-K12 genome using STAR (v.2.5.2b) with the following options: --outFilterMismatchNmax 2, --chimSegmentMin 15, --chimJunctionOverhangMin 15, --outSAMtype BAM Unsorted, --outFilterType BySJout, --alignMatesGapMax 1000, --outFilterScoreMin 1, --outFilterMultimapNmax 1. The following methods were applied to CUT&RUN experiments for SNF2H, and H3K27ac in MLS402, DL221, and SW872 cell lines. Tracks were created by using RPM normalized and spike-in adjusted bigWigs on UCSC genome browser. Regions of enrichment were identified using MACS2 (v2.1.2) using default parameters. ROE were annotated with a SPM score, and peaks with a score in the bottom 5% of SPM scores were not included in downstream analysis(16). The intersection of MSL402 SNF2H ROE and DL221 SNF2H was identified using bedtools (v2.28.0) with options -f 0.5 -r. Average line plot signal for SNF2H and H3K27ac was isolated using deepTools (v3.2.0). Heatmap signal shown was maxed out at 99th percentile across MLS402, DL221, and SW872 cell lines, and log2 transformed. The intersection of FUS-CHOP ChIP-seq ROE and SNF2H CUT&RUN ROE was identified using bedtools (v2.28.0). A permutation test was used to determine the significance of the FUS-CHOP SNF2H overlap.

SNF2H ROE were held constant, while the FUS-CHOP ROE were permuted by identifying size and chromosome matched random regions excluding unmappable regions. The intersection for each permutation was determined with bedtools (v2.28.0) with options -f 0.5 -r. The number of overlapping regions were stored for each iteration, and the p-value was calculated as the total number of permutations with an intersection > 863 over the total number of permutations (n = 1000).

RNA-seq Analysis

Adaptor sequences were trimmed using (cutadapt v1.12). Reads were then quality filtered using fastq quality filter in FASTX-Toolkit (v0.0.12) with options -Q 33, -p 90, and q 20. Reads were aligned to hg19 genome using STAR (v2.5.2b) with the following options: --quantMode TranscriptomeSAM, --outFilterMismatchNmax 2, --alignIntronMax 1000000, --alignIntronMin 20, --chimSegmentMin 15, --chimJunctionOverhangMin 15, --outSAMtype BAM Unsorted, --outFilterType BySJout, --outFilterScoreMin 1. Gene expression (TPM) was created using Salmon (v0.11.3). ERCC spike-in was performed, but not used in downstream analysis. Differentially expressed genes (MLS402/DL221 v. SW872) were identified using DESeq2 (v1.24.0). MA plots were created using Python.

Supplemental Information

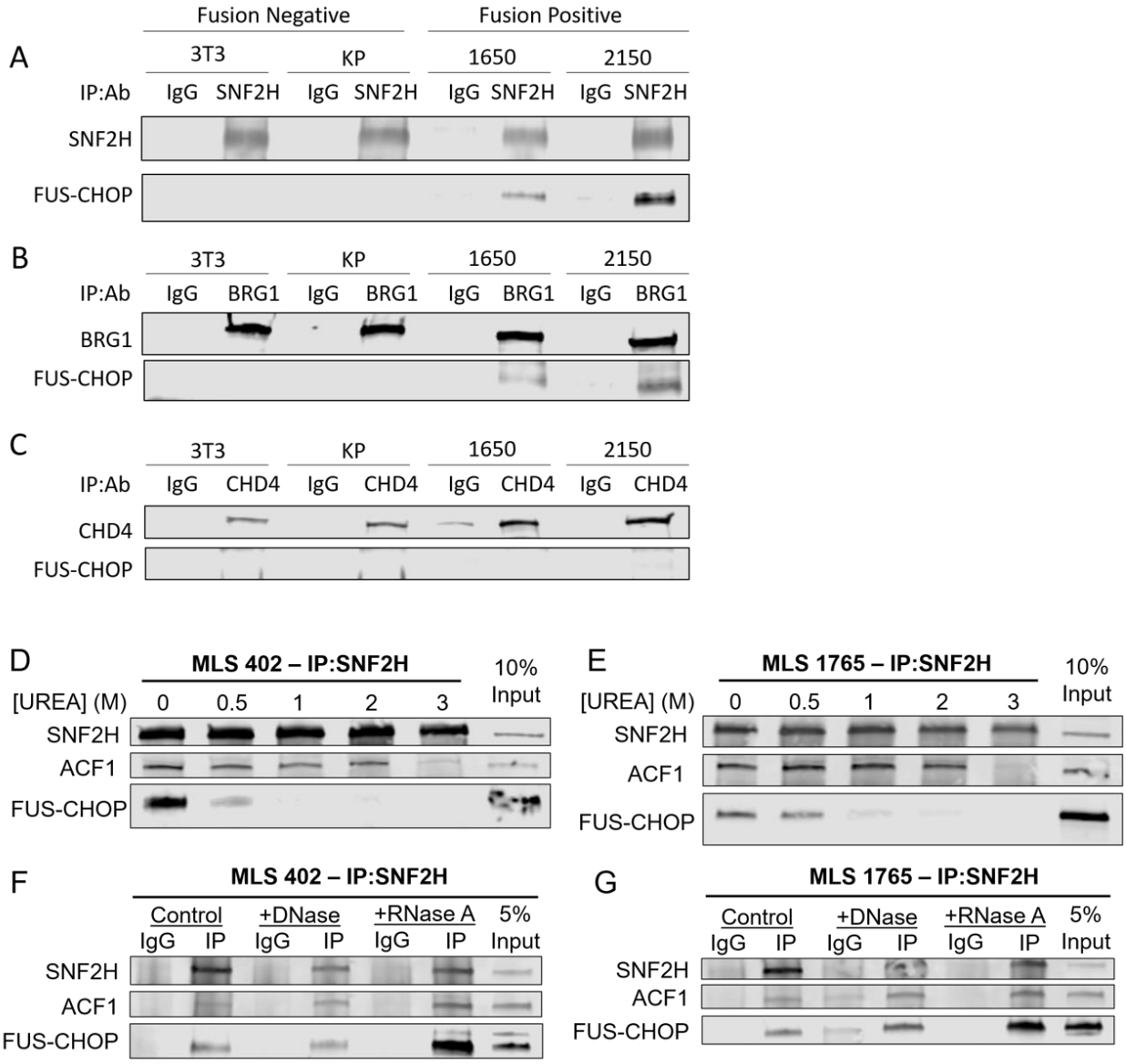

Fig. S1.

FUS-CHOP interacts with the ISWI and BAF complexes in mouse FUS-CHOP-driven sarcoma cell lines. (A) Snf2h, (B) Brg1, and (C) Chd4 co-IP for FUS-CHOP. 3T3 and KP cell lines are fusion negative. 1650 and 2150 are fusion-positive mouse sarcoma cell lines. (D) Urea denaturation assay in MLS402 and (E) MLS1765 cell lines performed with SNF2H co-IP for FUS-CHOP. ACF1 was used as a positive control for co-IP with SNF2H. (F) RNase/DNase assay in MLS402 and (G) MLS1765 cell lines performed with SNF2H co-IP for FUS-CHOP. ACF1 was used as a positive control for co-IP. Lysates were treated with either DNase or RNase A to deplete DNA and RNA in co-IP lysates, respectively. Representative images from two technical replicates are shown.

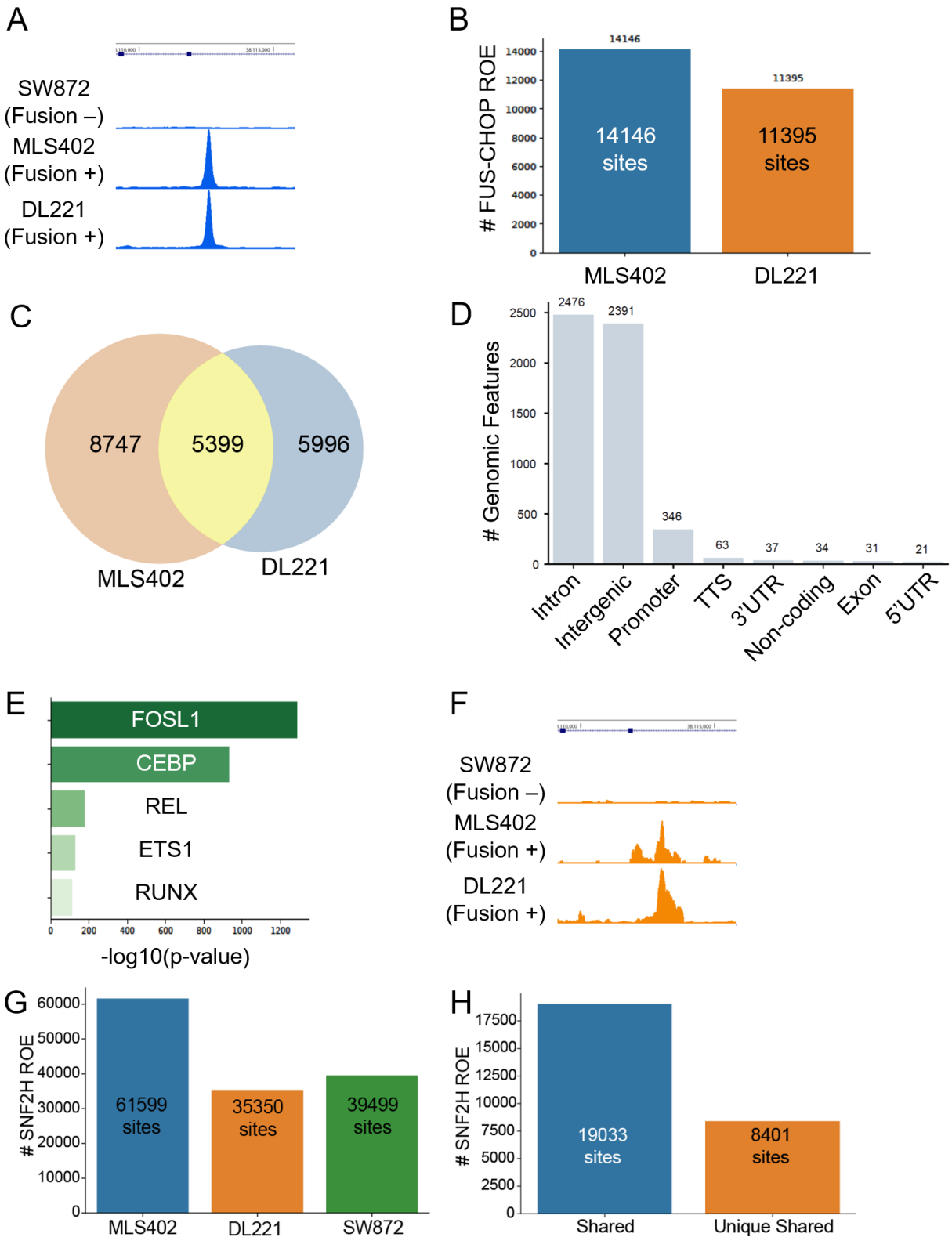
A
SW872
(Fusion –)
MLS402
(Fusion +)
DL221
(Fusion +)
B
FUS-CHOP ROE
14146
11395
14146
sites
11395
sites
MLS402
DL221
C
8747
5399
5996
MLS402
DL221
D
Genomic Features
2476
2391
346
63
37
34
31
21
Intron
Intergenic
Promoter
TTS
3'UTR
Non-coding
Exon
5'UTR
E
FOSL1
CEBP
REL
ETS1
RUNX
-log10(p-value)
F
SW872
(Fusion –)
MLS402
(Fusion +)
DL221
(Fusion +)
G
SNF2H ROE
61599
sites
35350
sites
39499
sites
MLS402
DL221
SW872
H
SNF2H ROE
19033
sites
8401
sites
Shared
Unique Shared

Fig. S2.

Genome-wide mapping of FUS-CHOP and SNF2H binding reveals widespread binding at enhancers and specific DNA-binding motifs in human MLPS cell lines. (A) Example track demonstrating FUS-CHOP transcription factor binding in human MLPS cell lines. (B) Total unique FUS-CHOP peaks called in MLS402 and DL221 cell lines. (C) Venn diagram showing the overlap of FUS-CHOP peaks in human MLPS cell lines. (D) Distribution of genomic features at MLS402-DL221 shared FUS-CHOP binding sites. (E) Top five DNA-binding motifs from motif analysis of unique FUS-CHOP peaks in human MLPS cell lines. (F) Example track demonstrating SNF2H binding in human MLPS cell lines. (G) Total unique SNF2H peaks called in MLS402, DL221, and SW872 cell lines. (H) Total shared SNF2H binding sites in MLS402, DL221, and SW872 cell lines, and total unique shared SNF2H binding sites in human MLPS cell lines only.

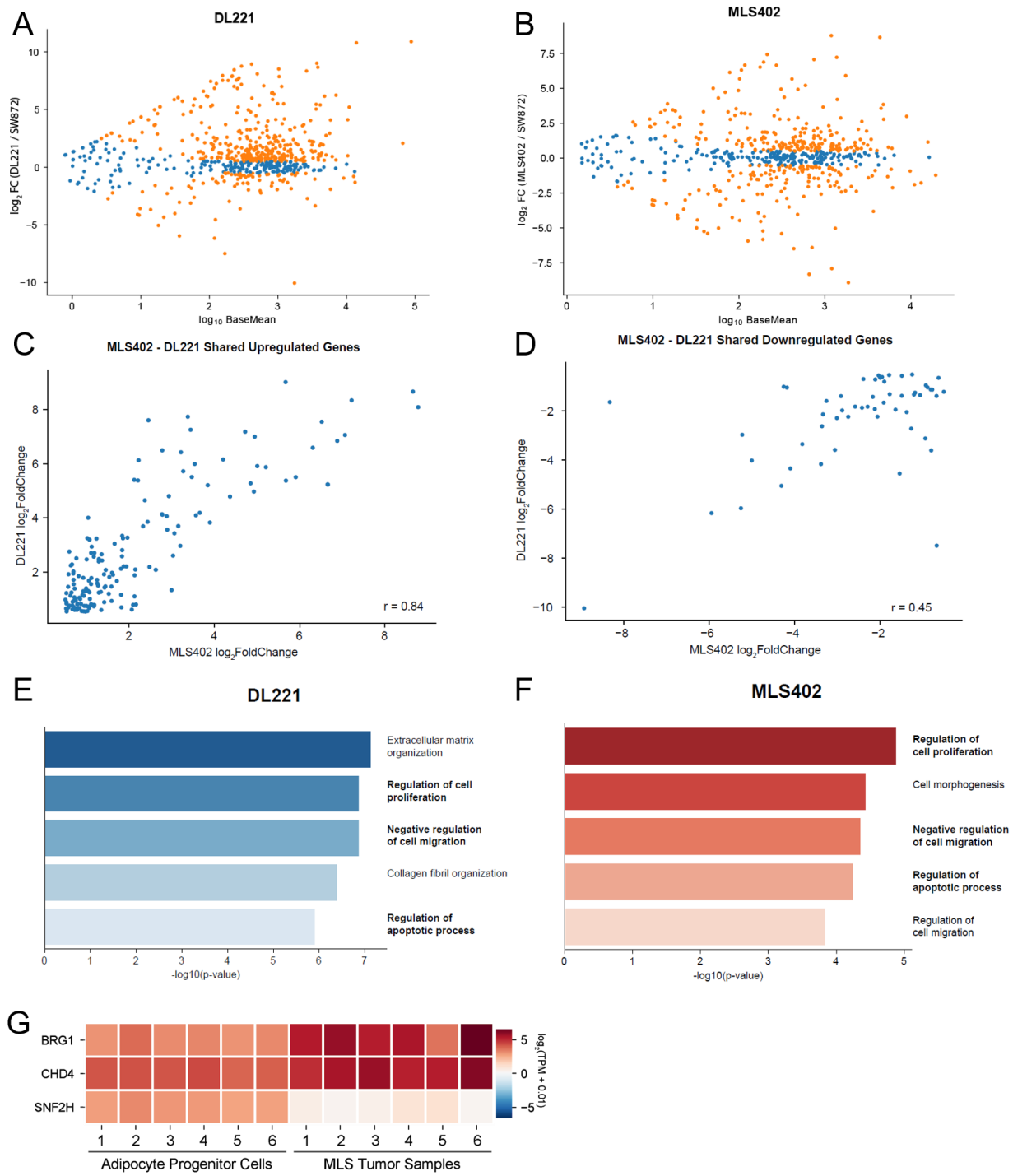

Fig. S3.

Transcriptome analysis of gene expression changes in human myxoid liposarcoma cells. (A) Differentially expressed genes in DL221 and (B) MLS402 MLPS cell lines compared to the SW872 liposarcoma cell line. Orange dots represent significant differential expression. Blue dots represent insignificant differential expression. (C) Scatterplot of upregulated genes in MLS402 versus upregulated genes in DL221. r = 0.84. (D) Scatterplot of downregulated genes in

MLPS402 versus downregulated genes in DL221. r = 0.45. (E) Enrichr gene ontology (GO) biological process results for upregulated genes in DL221 and (E) in MLS402 human MLPS cell lines. (G) Expression of chromatin remodeling complex proteins in human MLPS and adipocyte progenitor cells. A heatmap representation of gene-level RNA abundance levels for SNF2H, BRG1, and CHD4. Individual gene values are normalized to the median expression and log2 transformed for that dataset.

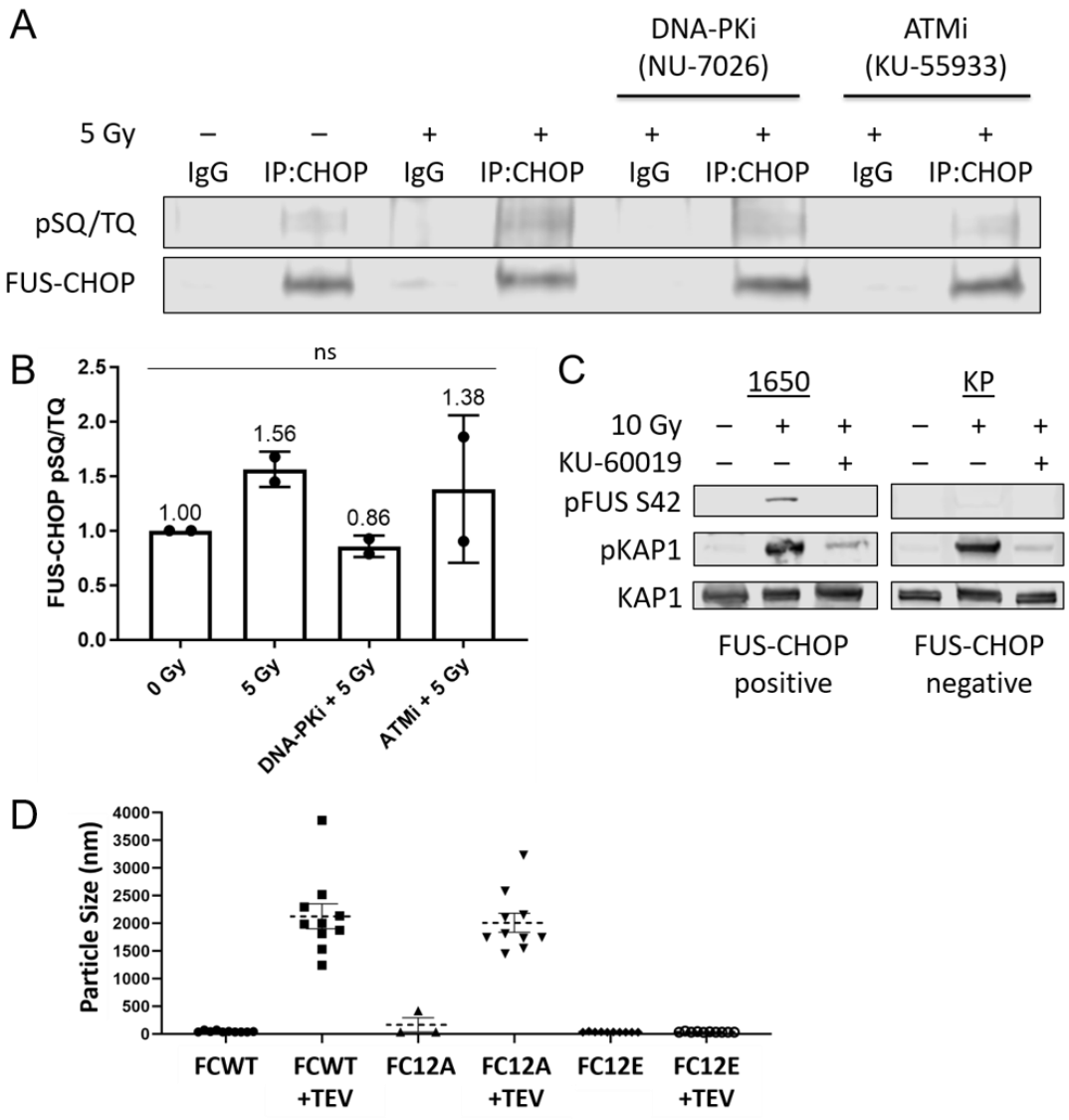

Fig. S4.

FUS-CHOP is phosphorylated after irradiation by DNA-PK and ATM. (A) IP of FUS-CHOP from MLS402 cell lines treated with no radiation, 10 Gy X-ray radiation, NU-7026 with radiation, and KU-55933 with irradiation. (B) Quantification of FUS-CHOP phosphorylation detected on immunoblot using a phospho-SQ/TQ antibody. ns = not significant, One-way ANOVA with multiple comparisons. (C) Immunoblot of phosphorylation at Ser42 in FUS-CHOP after irradiation and treatment with an ATM inhibitor, KU-60019. (D) FUS-CHOP (FCWT), FUS-CHOP 12A (FC12A), and FUS-CHOP 12E (FC12E) particle size before and after the addition of TEV protease to release the MBP solubility tag. Representative images from two technical replicates are shown.

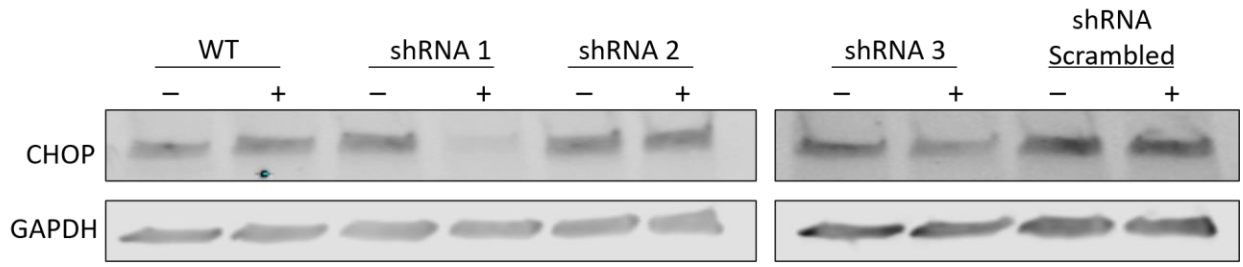

Fig. S5.

Validation of endogenous FUS-CHOP knockdown. Western blot shows protein knockdown 48 hours after dox-induction of shRNA targeting endogenous FUS-CHOP in MLPS wild-type cells (MLS 402).